10 GHz Low Loss Liquid Metal SIW Phase Shifter for Phased Array Antennas

Shaker Alkaraki, *Member, IEEE,* Quan Wei Lin, *Member, IEEE,* Alejandro L. Borja, *Member, IEEE,* Zhengpeng Wang, *Member, IEEE,* Hang Wong, *Senior Member, IEEE,* Shiyang Tang, Yi Wang, *Senior Member, IEEE,* James R. Kelly, *Member, IEEE*

***Abstract*— This paper presents a proof of concept demonstrator for a pair of novel phase shifters based on substrate integrated waveguide (SIW) technology. Gallium-based liquid metal (LM) is used to reconfigure each phase shifter. The paper presents LM phase shifters that, for the first time, have a phase shifting range of 360°. The phase shifters have a small electrical size, and they are intended for use within phased array antenna applications. The paper also presents a design procedure for the phase shifters. The procedure has been used to design two phase shifters operating at 10 GHz. The design process can be readily scaled for operation at other frequencies. The proposed phase shifters are reciprocal and bidirectional and they have very low insertion loss. A series of reconfigurable LM vias are used to achieve the phase shift. Each of LM via is activated once a drill hole is filled with LM and it is deactivated once LM is removed. Using this method; it is possible to achieve a phase shift step ranging from 1° to 100° using a single LM via. Moreover, the overall phase shift can be extended to 360° by employing several LM vias in series inside the SIW. The proposed phase shifters have an insertion loss lower than 3 dB and provide a total phase shifting range of approximately 360° in eight steps of approximately 45° each. This enables the proposed two phase shifters to have an extraordinary Figure of Merit (FoM) of 131.3 °/dB and 122.4 °/dB.**

***Index Terms*— Phase shifter, phased arrays, liquid metal, reconfigurable circuit, SIW.**

I. Introduction

Varoius microwave and millimeter-wave (mm-wave) systems rely on using phase shifters. This includes microwave instrumentation, antennas capable of electronic beam scanning, modulators, and smart antennas. One of the main disadvantages of state–of-the-art phase shifters, operating at microwave and mm-wave frequencies, is that they have high insertion losses (IL). Phase shifters have been traditionally developed using several approaches including: 90 -hybrid couplers [1], switched transmission lines [2], periodic loaded lines [3] and unequal-length unequal-width transmission line [4]. However, although these phase shifters offers large phase shift and high performance, their large physical size makes them impractical for use in compact phased array systems [5]. Some of the most the widely used phase shifters are those based on PIN diodes and GaAs FETs [6]-[8]. However, these phase shifters have several limitations. Phase shifters based around GaAs FETs have lower IL than competing devices but have limited radio frequency (RF) power handling capability [6]-[8]. Phase shifters based around PIN diodes have higher RF power handling capability. However, they suffer from relatively high IL losses. Some other widely used phase shifters rely on CMOS technology to achieve high resolution and accuracy [5], [9]-[16]. CMOS phase shifters are small in size and can be used in integrated circuits (ICs) [5], [9]-[16]. However, the main drawbacks of CMOS phase shifters are they have losses in amplitude, limited output power and relatively poor noise figure due to the high insertion loss and nonlinearity. For instance, the typical IL performance for a state-of-the-art CMOS based active phase shifter is much higher than 10 dB at 10 GHz [10]-[12], [15]-[17].

Other less common technologies that have been used to design phase shifters at X-band include Liquid crystal and Ferroelectric Ceramics. However, Ferroelectric phase shifter have seen limited use due to: the complexities involved in their fabrication, their high ILs [18]-[22], and their limited phase shifting performance [23]-[25]. For instance, the Ferroelectric phase shifter in [18] has an IL of 6.6 dB with a measured phase shift of 342° at 10 GHz and the Ferroelctric based phase shifter in [21] has an IL of 10.3 dB at 10 GHz. However, the phase shifters in [23]-[25] have a limited phase shifting range; 166° for [21], 200° for [24], and 216° for [25]. On the other hand, Liquid crystal (LC) materials are mostly used to design high performance phase shifters at mm-wave and THz frequencies. At these frequencies modern LC materials have low IL together with wide phase tuning range [26]-[40]. However, LC materials have seen very limited usage at lower frequencies (i.e. below

This work was supported in part by a grant from The United Kingdom Engineering and Physical Research Council, EPSRC, under grant number: EP/P008402/1, EP/P008402/2, and EP/V008420/1 (Corresponding author: Shaker Alkaraki.).

Shaker Alkaraki and James Kelly are with The Antennas & Electromagnetics Research Group, The School of Electronic Engineering and Computer Science, Queen Mary University of London, Mile End Road, London, United Kingdom (email: {s.m.alkaraki,j.kelly}@qmul.ac.uk).

Alejandro L. Borja is with the Departamento de Ingeniería eléctrica, electrónica, automática y comunicaciones, Escuela de Ingenieros Industriales de Albacete, Universidad de Castilla-La Mancha, Campus Universitario, ES 02071 Albacete, Spain (e-mail: alejandro.lucas@uclm.es).

Quan Wei Lin and Hang Wong are with The State Key Laboratory of Terahertz Millimeter Waves, Department of Electrical Engineering, City University of Hong Kong, Hong Kong (e-mail: {qwlin2, hang.wong}@cityu.edu.hk).

Zhengpeng Wang is with the school of Electronics and Information Engineering, Beihang University, Beijing, China. (wangzp@buaa.edu.cn)

Shiyang Tang and Yi Wang is with the University of Birmingham, Birmingham, United Kingdom({s.tang,y.wang.1}@bham.ac.uk).

30 GHz) [26]-[40]. This because a greater thickness of LC material is required at lower frequencies which leads to higher IL and limited phase tunability range. For example, the phase shifter in [41] can provide a phase shift only up to 185° between 14.5 GHz and 15.3 GHz and the LC based phase shifter in [42] provides a measured phase shift of ≈101° and IL of ≈5 dB at 10 GHz. Furthermore, the two LC based phase shifters, in [43] provide a phase shift up to 215° with an IL, at 10 GHz, of 16 dB and 9 dB, respectively. Other LC based phase shifter, in [44] and [27] have a maximum phase shift of ≈100° for [44] and phase shift of ≈60 for [27] with IL of ≈ 3.9 dB for [44] and IL of 2.5 dB for [27] at 10 GHz.

[5]-[12], [15]-[25], [41]-[66] report Phase shifters operating at 10 GHz. Those phase shifters have an average IL performance of 6.35 dB. The phase shifters considered are based on a very wide range of different technologies. For example, phase shifters based around MEMS-switched capacitors offer relatively low IL level at X-band frequencies (i.e. [66] has an IL of 6 dB at 10 GHz). However, MEMS have several disadvantages which have prevented their large-scale usage. For instance, MEMS suffer from contact welding which degrades their reliability [45], [50]-[51], [63], [66].

Significant efforts have been made by researchers in the field to develop high performance phase shifters having low-loss and reduced size. One of the figure-of-merit (FoM) which is widely used to compare phase shifters [25], [27], [35], [42], [44], [67] is given in (1).

$$FoM = \frac{\Delta\emptyset_{max}}{IL_{max}} \quad (1)$$

Where, $\Delta\emptyset_{max}$: is the maximum phase shift and IL_{max} is the maximum insertion loss, at particular frequency.

Recently, there has been growing interest in using Gallium based Liquid metal (LM) to make reconfigurable circuits and devices. This includes: microwave filters [68]-[71], Radio Frequency (RF) switches [72]-[74], antennas [75]-[78], and phase shifters [79]-[80]. [79] presents a phase shifter based on a defected ground plane and it can be reconfigured using LM. The phase shifter operates at 5.6 GHz and achieves a total phase shift of only 67.2°. The phase shift can be varied in uneven steps. The phase shifter has a FoM of 70°/dB [79]. The approach in [79] is interesting, but more work is needed to obtain a wider phase shifting range in even steps. The phase shifter in [80] achieves a total phase shift of 180° with peak FoM of 78.3°/dB at 10 GHz. The phase shifter employed the switched line approach. It relies on a series of LM vias to switch between several SIW transmission lines having different electrical lengths. A series of vias are used to provide fine control of the phase shift. However, the overall phase shift provided by this approach is limited to 180°. Also the bandwidth of the phase shifter is relatively narrow. In addition, phase shifters employing the switched line approach e.g. [80] tend to have a relatively large physical size. [80] has a complex design due to the large number of LM vias used to change the direction of the electromagnetic waves between different paths. These characteristics would be disadvantages when attempting to integrate the phase shifter with other circuitry e.g. the feeding structure associated with a phased array antenna.

This paper proposes two phase shifters that can be reconfigured using liquid metal and are suitable for integration in a phased array based around an SIW feeding structure. The proposed phase shifters are the first such phase shifters having a tuning range of up to 360° together with a very low IL and a small electrical size. For example, the proposed phase shifters have FoM values of 131.3 °/dB and 122.4 °/dB at 10 GHz. These are very high FoM values and to our knowledge, these are amongst the highest FoM figures reported for a 10 GHz phase shifter. One of the other main advantages of the proposed phase shifters is that their total electrical length is relatively small, which makes it easier to integrate them in an SIW feeding network to realize a beam scanning phased array. Also, we hypothesize that the proposed phase shifters will be able to handle very high RF power. The reason for this is that there seems to be nothing about LM that might restrict its RF power handling ability. For this reason the RF power handling ability of the SIW phase shifter will be limited only by the SIW transmission line itself, which is considerable. We anticipate that the proposed phase shifters will provide remarkably enhanced linearity performance [75]. However, in comparison with phase shifters based around competing technologies, the proposed phase shifters have a relatively narrow operating frequency bandwidth together with a relatively coarse resolution, of 45°, and a relatively large physical size. Furthermore, it is estimated that the proposed phase shifters have a reconfiguration time ranging from 3 milliseconds to seconds, depending on the technique used to actuate the LM [55], [81]. The proposed phase shifters are suitable for applications requiring low loss and high power-handling capabilities.

The same design concept can also be employed to create phase shifters operating at millimeter wave frequencies. Currently there are no off-the-shelf electronically controllable phase shifters operating at frequencies above 40 GHz.

The paper is organized as follows. Section II presents the structure of the proposed LM phase shifter. Section III discusses the theory, concept and the design process for the proposed phase shifters. Section IV explains the considerations involved in fabricating the phase shifters. Section V presents the experimental and simulated results. Section VI, provides overall conclusions.

II. Concept and Theory of the Phase Shifter

It has been proven that a phase shift is produced when a high pass filter is used in a topology known as the switched high-pass/low-pass [82]-[85]. Such a filter can be realized using a variety of different technologies. One such technology which is studied in detail in [82], [85]-[87] is a cylindrical conductive post, or an array of posts, in a rectangular waveguide, as shown in Fig. 1. This conductive post is equivalent to a via in an SIW transmission line. The horizontal position (s) of the post as well as the post diameter are used to control the realized phase shift. Furthermore, it is possible to represent a single metal post as a high pass filter consist of T-network of lumped elements. The phase shift (φ) is controlled by the susceptance B and the

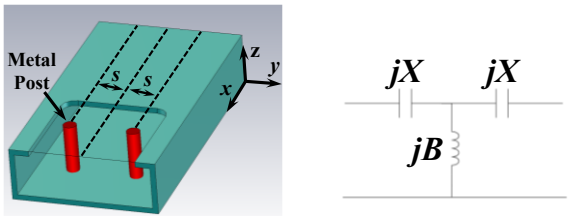

(a) (b)

Fig. 1. The schematic of conductive posts in a rectangular waveguide with the equivalent circuit. (a) Rectangular waveguide, and (b) equivalent circuit for a single post.

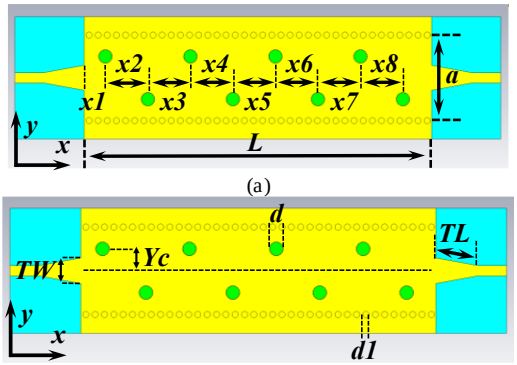

(a)

(b)

Fig. 2. The prototype of the Liquid metal based phase shifter. (a), (b) Top view and (c) photos of the prototype. Key: copper = yellow, substrate = light blue, copper plated vias = yellow, LM vias = green.

TABLE I
THE PHASE SHIFTER'S DIMENSION (UNIT: MM)

$x1 = 2.6$	$x2 = 6.7$	$x3 = 5.7$	$x4 = 6.2$
$x5 = 6.1$	$x6 = 6$	$x7 = 6.3$	$x8 = 6.2$
$a = 14$	$L = 57.2$	$d = 1.8$	$d1 = 1$
$TL = 6.8$	$TW = 4.1$	$Yc = 3$	$x1 = 7$

reactance X as given in (2) [82], [84].

$$\varphi = \frac{B + 2X - B\,X^2}{2(1 - 2BX)} \qquad (2)$$

Based on Eq.2 and the above discussion, a substrate integrated waveguide (SIW) phase shifters are developed. The phase shifters operate at 10 GHz as it is the Centre of X-Band. The schematics of the proposed phase shifter is shown in Fig. 2. The proposed phase shifter has eight liquid metal (LM) vias with vias diameter (d). The phase shifter dimensions are shown in Table. I.

In fact, adding a single via in an SIW transmission line will create a phase shift that is directly proportional to the vias diameter (d) and inversely proportional to the distance between the centre of the SIW and the position of the via with respect to the y-axis (Yc). A single via will cause a phase advance in the phase of an electromagnetic (EM) wave propagating in the SIW, as shown in Fig. 3. In other words, adding the via will reduce the electrical length of the SIW transmission line. This results in a shorter path for the wave that naturally causes an advance in the phase of the EM wave. Adding an array of vias will further reduce the electrical length of the SIW, as shown in Fig. 4 and it will increase the phase advance, resulting in a greater phase shift that can be controlled using the distance, in the x-axis direction, between the vias.

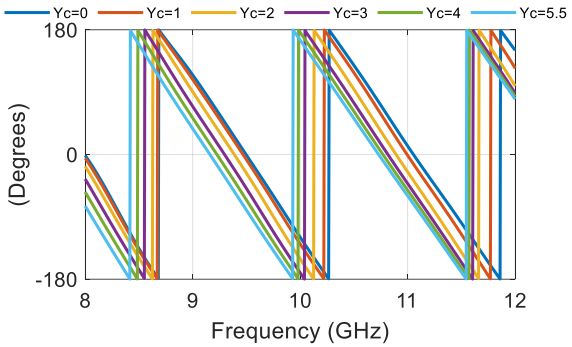

Fig. 3. Effect of Yc on the phase of the proposed phase shifter at 10 GHz for a fixed via diameter of 1.8 mm.

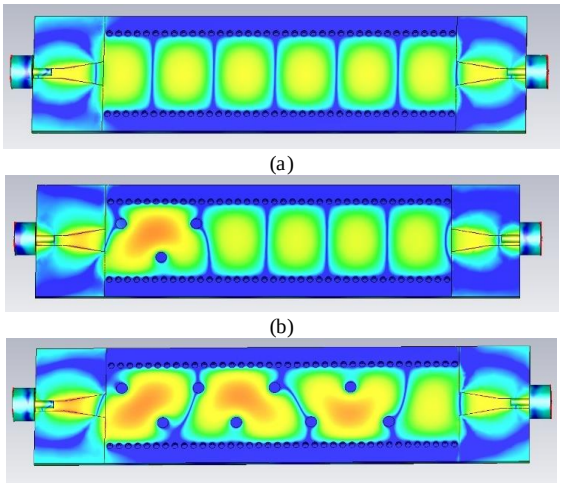

(a)

(b)

(c)

Fig. 4. The electric field distribution inside the proposed phase shifter at 10 GHz with/without the presence of LM vias. (a) With no vias, (b) with three LM vias and (c) with eight LM vias

When the vias are empty of LM the via size has a negligible effect on the RF performance of the phase shifter provided that the via diameter is less than 2mm. When the vias are filled with liquid metal they can control the phase shift, provided by the phase shifter. Given that the width of the SIW line (a) is fixed, the phase shift and the insertion loss (IL) contributed by a single LM via can be controlled by altering the horizontal position of the via (denoted Yc), as well as by the via diameter (denoted d), as shown in Figs. 5 to 7. Note that, in order to achieve the maximum phase shift per via, that particular via must have larger diameter and it must be moved along the y-axis of the SIW transmission line such that it is closer to the origin of the y-axis. For a fixed via diameter, the phase shift contributed by each via is thus inversely proportional to Yc. For a particular application we may prefer to set the diameter of the vias to be larger or smaller. We can then alter Y_c to compensate for the difference in phase shift that would otherwise result. Consider the case where $a = 14$ mm and the via diameter is set to 2 mm. For this combination of parameters, a phase shift ranging from 7.8° to 88.8° could be obtained using a single via, by gradually changing Yc from 5.5 mm to 0 mm, as shown in Fig. 6(a). In addition, when the via diameter is 0.5 mm a single via can provide a phase shift of up to 38.4°. When the via diameter is 3 mm, on the other hand, a single via can provide a phase shift of 117°, as shown in Fig. 6(a). However, the insertion loss increases in proportion to the amount of phase shift provided by

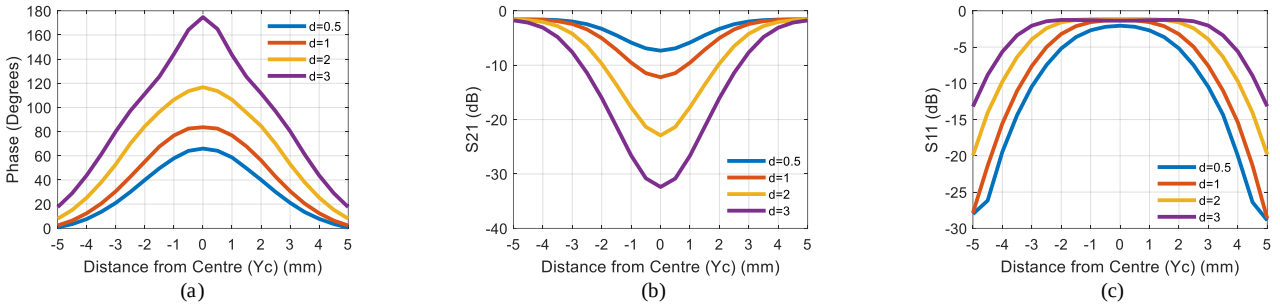

(a) (b) (c)

Fig. 5. The effect of Yc on the phase shift and S-parameters when a = 11mm at 10 GHz. (a) S_{21} phase, (b) amplitude of S_{21} and (c) amplitude of S_{11}.

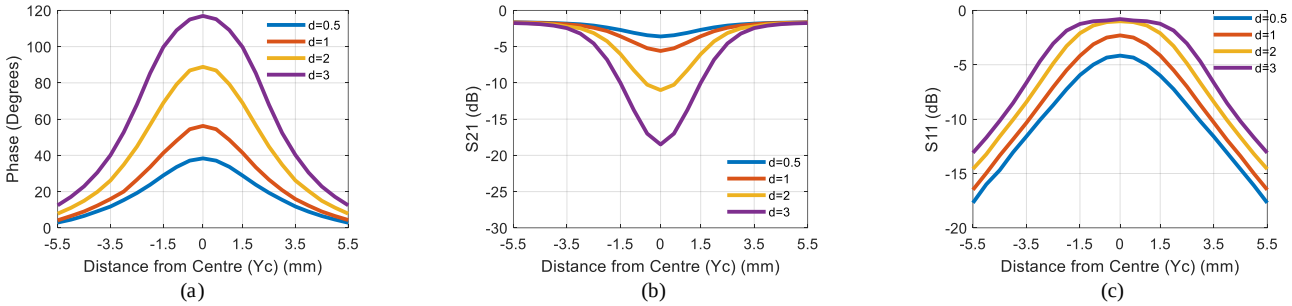

(a) (b) (c)

Fig. 6. The effect of Yc on the phase shift and S-parameters when a = 14mm at 10 GHz. (a) S_{21} phase, (b) amplitude of S_{21} and (c) amplitude of S_{11}.

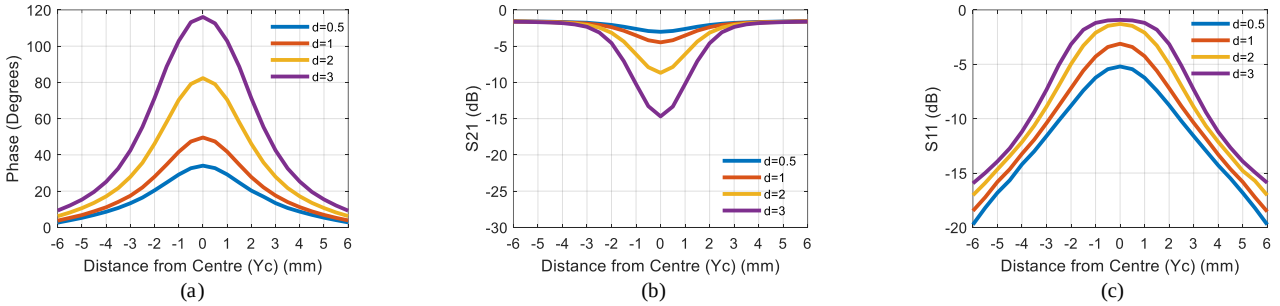

(a) (b) (c)

Fig. 7. The effect of Yc on the phase shift and S-parameters for when a = 15.4 mm at 10 GHz. (a) S_{21} phase, (b) amplitude of S_{21} and (c) amplitude of S_{11}.

each via, as shown in Figs. 5(b), 6(b), and 7(c). This insertion loss can be attributed to mismatch, as shown in Figs. 5(d), 6(d), and 7(d). For example, consider the case introduced above, where a = 14 mm and when d = 2 mm, the IL is 1.7 dB when Yc = 5.5 mm. However, the IL rises to 2.47 dB when Yc = 3 mm, to 4.25 dB when Yc = 2mm, and to 11 dB when Yc = 0 mm, as shown in Fig. 6 (b). Furthermore, the IL ranges from 1.7 dB to 3.6 dB, when d = 0.5 mm and from 1.75 dB to 18.5 dB when d = 3 mm as shown in Fig. 6(b).

For a given value of Yc and via diameter (d) the maximum phase shift achieved by a single via is inversely proportional to the width of the SIW line (a). Reducing the width of the SIW line thus results in a larger phase shift per via, as shown in Figs. 5 (a) to 7(a). For example, when a = 11mm the phase shifter provides a maximum overall phase shift of 174.8°, as shown in Fig. 5(a). while the maximum phase shift is 117° when a = 14mm, as shown in Fig. 6(a) and it is 115°, when a = 15.4 mm. However, the insertion loss (IL) increases as the width of the SIW line is reduced, due to an increase in the level of mismatch and thus reflection. For example, the worst reflection performance and thus IL is obtained when a = 11mm, as shown in Figs. 5(b) and 5(c). The width of the SIW line (a) also affects the upper and lower cut off frequencies of the SIW transmission line, as explained in Eqs. 3 and 4 [88]-[90].

$$F_{C,mn} = \frac{c}{2\sqrt{\varepsilon_r}}\sqrt{\left(\frac{m}{a}\right)^2 + \left(\frac{n}{b}\right)^2} \quad (3)$$

$$F_{C,m0} = \frac{mc}{2a\sqrt{\varepsilon_r}} \quad (4)$$

where: c is the speed of light in a vacuum, m and n are integers and b is the height of SIW transmission line.

Specifically, the cut-off frequencies of the TE_{10} and TE_{20} modes, propagating in the SIW line, are controlled by the width of the SIW transmission line (a). Please note that TE_{10} is the fundamental mode within the SIW line. The operation frequency of the proposed phase shifter was set to 10 GHz. 10 GHz corresponds to the center of X-band. The width of the SIW line (a) is chosen to be 14mm ($< \frac{\lambda}{2}$ where λ is the free-space wavelength at the operating frequency i.e. 10 GHz). This would enable the proposed phase shifter to be easily integrated within the feeding structure of a phased array antenna. In phased array antenna systems, the antenna elements are typically separated by $\approx \frac{\lambda}{2}$ to yield an optimum compromise between the steering range and grating lobe performance [91]. In the proposed design, the full width of the proposed phase shifter, including the copper vias is 15mm, which is $\frac{\lambda}{2}$ at 10 GHz.

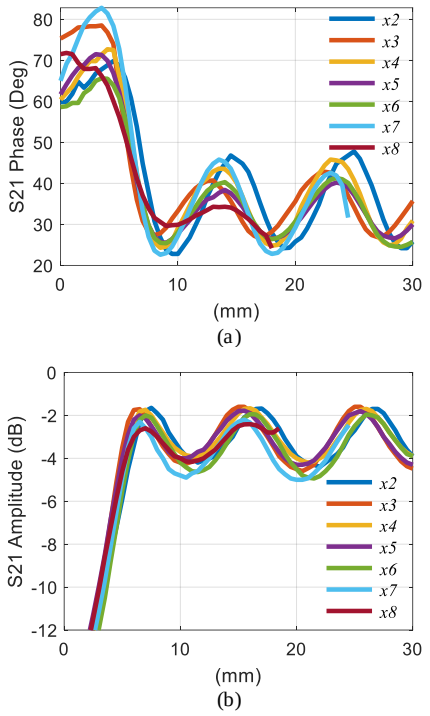

Fig. 8. The effect of the horizontal separation (*x2 to x8*) between the LM vias on the S_{21} of the proposed phase shifter at 10 GHz. (d =1.8 mm and Yc =3 mm) (a) Phase and (b) amplitude.

According to Eqs. 3 and 4, when a =14 mm, the lower cut-off frequency is 5.7 GHz, while the upper cut-off frequency is 11.6 GHz. Please note that the bandwidth of the phase shifter is principally controlled by the upper cut off frequency. Above this frequency higher order modes will propagate inside the SIW line, which is undesirable. Increasing the width of the SIW line would have the effect of reducing the upper cutoff frequency and thus the bandwidth of the phase shifter. For example, When a = 15.4 mm, the upper cut-off frequency of the SIW line is 10.3 GHz. In addition, narrower transmission line which has a width of less than 14mm have higher cutoff frequencies and achieves higher phase shift per LM via as discussed previously (i.e. lower and upper cut off frequencies are 7.2 GHz and 14.5 GHz, when a = 11 mm). However, SIW with narrower transmission line width has worst insertion loss and they are much smaller than $\frac{\lambda}{2}$ at 10 GHz.

The total phase shift, provided by the phase shifter, can be increased by adding more LM vias. The exact value of the phase shift and the IL can be controlled by the horizontal distance between two LM vias in the x-axis direction (*x2 to x8*), as shown in Fig. 8. For example, the addition of a second LM via yields a phase shift of between 22.5° and 58°. The amount of phase shift provided is independent of which of the 7 remaining LM vias are activated, as shown in Fig. 8(a). In principle, therefore, it is possible to design a reconfigurable phase shifter with eight LM via that can achieve a phase shift of up to 360°. In addition, there is no advantage to the particular starting position chosen for the LM via. Both positions of Y_c (i.e. whether the first via is offset in the +y-axis direction or the –y-axis direction, with respect to the origin of the y-axis) yield the exact same performance as shown in Fig. 6. The phase shifter can have 9 states and a step of ~45°, as summarized in TABLE. III. Finally, it is possible to design the phase shifter with non-alternating via positions (i.e. all vias are on one side of the waveguide). However, this will yield to lower phase shift achieved by each via and will increase the IL. For example, The maximum phase shift can be achieved using this methodology is ≈260° when 8 vias are used with a maximum phase shift of around 32°. This is significantly much less than the total phase shift can be achieved when using alternating vias as proposed in our design shown in Fig. 2.

TABLE II
THE OPERATING STATES OF THE PHASE SHIFTER

State	Number of Active LM Via	Total Phase shift
State 1 (S1)	0	0
State 2 (S2)	1	45°
State 3 (S3)	2	90°
State 4 (S4)	3	135°
State 5 (S5)	4	180°
State 6 (S6)	5	225°
State 7 (S7)	6	270°
State 8 (S8)	7	315°
State 9 (S9)	8	360°

III. Design Criterion for the Proposed Phase Shifter

This section will describe a methodology that should be followed in order to design the proposed phase shifters. We present two different versions of this methodology corresponding to the two proposed LM phase shifters. The design process, described in [88]-[90] and Eq. 3 and Eq. 4 were used to determine the width of the SIW transmission line (a) as discussed in the previous section. Next a tapered transition from microstrip to SIW is designed. A copy of that transition was added to each side of the SIW transmission line. Each of the microstrip lines were then terminated in an SMA connector. The design criterion in [89], [92] was used to design the tapered transition. The Frequency Domain Solver in CST Microwave Studio® 2019 was used to optimize the length and width of the transition (*TL* and *TW*). After that, the phase shift is controlled by adding LM vias. We can envisage two possible design methodologies and these result in the two phase shifter designs proposed in this paper. The first methodology involves maintaining a non-uniform distance, in the x-axis direction, between LM vias. In this case the required phase shift per via is controlled by the horizontal distances between the LM vias, labeled $x2$ to $x8$. The second design methodology involves maintaining a uniform distance, in the x-axis direction, between the vias (i.e. $x = x2 = x3 = x4 = x5 = x6 = x7 = x8$). We then optimize x to achieve a total phase shift of 360°. The following sub-sections discuss these design methodologies in detail.

A. Phase shifter design with non-uniform distance between the LM vias

The following text summarizes the procedure for designing the non-uniform phase shifter.:

1. Determine the dimensions of the SIW using (3) and (4).
2. Add the first LM via and optimize its position in the y-axis (*Yc*) direction, in order to achieve the required

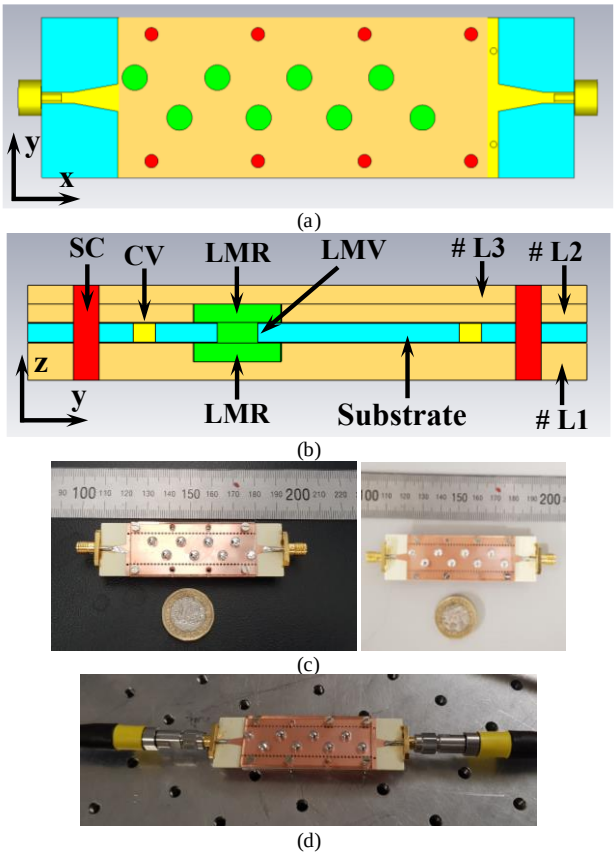

Fig. 9. The schematics of the fabricated phase shifter. (a) Top view with Perspex cover and (b) cross section of z-y plane, (c)–(d) prototypes of the proposed phase shifter. Key: L#1 = first layer of Perspex, L#2 = second layer of Perspex, L#3 = Third Layer of Perspex, LMR = reservoir holding Liquid metal (LM), LMV = Via consists of LM, CV = Copper via, SC = Metallic Screw, Substrate = light blue, Copper plated vias = yellow, Perspex = Orange, Metallic Screw = red, LM vias = green.

phase shift. Please note that $x1$ has no effect on the phase shift. The phase shift is mainly controlled by Yc. For the proposed phase shifter Yc was set to 3 mm in order to achieve a phase shift of 31°. This particular value of phase shift was chosen in order to keep the IL below 2.4 dB at 10 GHz.

3. Add the second LM via and optimize the distance (i.e. $x2$) between both LM vias in order to achieve a phase shift of 47° at 10 GHz.
4. Repeat step 3 for the rest of LM vias (i.e. the third via to the eighth via by optimizing parameters $x2$ to $x8$). $\approx 47°$ was selected as value of phase shift for those vias, so that the total phase shift achieved by the eight LM vias is 360°. ($31° + 47° \times 7 = 360°$).

B. Phase shifter design with uniform distance between the LM vias

The uniform phase shifter is simpler to design than the non-uniform phase shifter. However, this is at the cost of higher IL and reduced accuracy in controlling the size of the smallest phase step. The following text summarizes the procedure for designing the non-uniform phase shifter:

1. Determine the dimensions of the SIW using (3) and (4).
2. Add the first LM via. Please note that $x1$ has no effect on the phase shift. The phase shift is mainly controlled by Yc. For the proposed phase shifter Yc was set to 2.7 mm in order to keep IL below 3 dB at 10 GHz. This value of Yc yields a phase shift of 35°.
3. Add the rest of the LM vias. All vias are added at the same time. The horizontal distance between the vias is maintained constant and it is labelled x ($x = x2 = x3 = x4 = x5 = x6 = x7 = x8$). Next, x is optimized through a parametric study and selected to be 7 mm, so that the entire phase shifter achieves a phase shift of around 360° using only eight LM vias.

IV. Fabrication Considration

The hardware prototype was fabricated and actuated as shown in Fig. 9. The phase shifters are designed using SIW technology and fabricated on a RO4003C substrate with a thickness (h) of 0.813mm. The tangent loss of the substrate is 0.0027 and the dielectric constant is 3.55. The prototypes of the phase shifter were fabricated using chemical etching technology which is a standardized procedure for fabrication of printed circuit boards (PCB).

LM was contained and guided in a channel structure consists of Perspex. The channel consisted of three layers of clear Perspex, as shown in Fig. 9. Layers 1 (#L1) and layer 2 (#L2) contains reservoirs used to hold liquid metal (these are referred to as LMRs), while layer 3 (#L3) is used as a cover. Eight metallic screws (SC) located outside the SIW are used to hold the different layers of Perspex together, as shown in Fig. 9. The screws have no effect on the RF performance of the proposed phase shifters because they are located outside the SIW transmission line. LM is injected into and removed from the drill holes using a syringe. This actuation approach is commonly used and literature contains several papers, which adopt this approach for actuation [76], [93]-[102]. Several other actuation techniques are reported in literature such as: 1) the use of a micropump [55], [64], [81], [103]-[104] or 2) the use of electrochemically controlled capillary action [105]-[106]. However, LM actuation is not within the scope of the research reported in this paper. It would be possible to adopt any of these techniques to actuate the proposed phase shifters, as changing the method of actuation will have no effect of the RF performance of the phase shifters. This is because that the actuation circuits could be placed above or below the ground plane of the phase shifter, where the strength of magnetic field (H-field) and electric field (E-field) are extremely low. In addition, the diameter (d) was set to 1.8 mm to make it easier to fill and empty the holes with liquid metal (LM) smoothly and repeatedly. In our experience, it is technically possible, but difficult to fill vias with LM if they have a diameter of less than 0.9 mm. However, it is easier to fill vias having a diameter larger than 0.9 mm. Larger vias have a much larger area. For example, a via with a diameter of 1.8 mm has an area that is almost four times larger than that of a via with a diameter of 0.9 mm. Furthermore, simulation results show that the via size has limited effect on the RF performance of the phase shifter. Vias with a diameter of less than 2 mm are electrically small at 10 GHz and the radiation and RF power leakage from them is negligible. A via size between 1 mm and 2 mm is thus

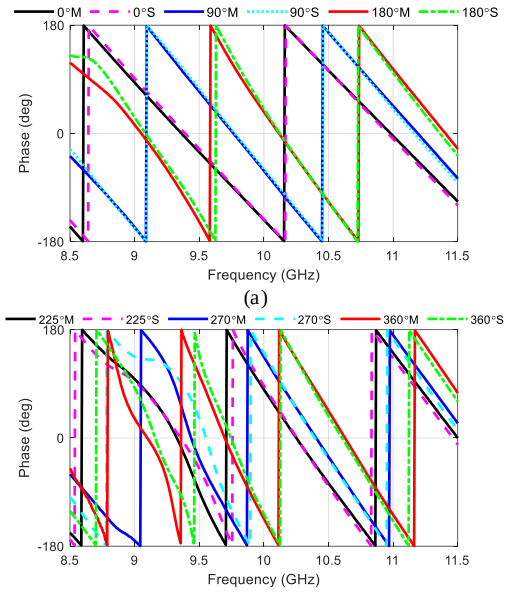

Fig. 10. The measured S_{21} of the proposed non-uniform LM phase shifter. (a) 0° to 180° and (b) 180° to 360°. [M: is for measurement results and S is for simulated results]

TABLE III.
MEASURED PHASES OF THE PROPOSED NON-UNIFORM LM PHASE SHIFTER AT 10 GHZ

State (S)	Number of active LM vias	Simulated total phase shift (step)	Measured total phase shift (Step)	Measured IL (dB)
(S1)	0	NA	NA	1.7
(S2)	1	30.5° (30.5°)	31.2° (31.2°)	2.3
(S3)	2	77.8° (47.3°)	81.8° (50.6°)	1.9
(S4)	3	125.3° (47.5°)	132.3° (50.5°)	1.9
(S5)	4	172.7° (47.4°)	179° (46.7°)	2.0
(S6)	5	219.5° (46.8°)	223.8° (44.8°)	2.1
(S7)	6	267° (47.5°)	277.9° (53.1°)	2.8
(S8)	7	313.9° (46.9°)	323.4° (46.5°)	2.3
(S9)	8	360.5° (46.6°)	367.6° (44.2°)	2.8
	Total	360.5	367.6	

recommended for the proposed application and the main advantage of using larger vias is that they are easier to fill with LM. However, using a via diameter larger than 2mm will introduce excessive IL, when the vias are empty of LM. For instance, an extra 0.25 dB of IL results when the via diameter is increased from 2 mm to 3mm. Furthermore, after removing LM from the vias we noticed that no residues remained. Moreover, we typically use the liquid metal several time to actuate the phase shifters and we have found that this does not affect the RF performance of the phase shifters.

V. EXPERIMENTAL RESULTS

Two phase shifters were fabricated and measured. Both phase shifters achieve a phase shift up to 360°. In the first phase shifter there is a non-uniform distance between the LM vias and in the second phase shifter there is a uniform distance between the LM vias.

A. Phase shifter with non-uniform distance between the LM vias

The proposed phase shifter achieves a phase shift of up to 360°, with eight different steps, depending on the number of active LM vias. Figs. 8 and 9 show the simulated and measured

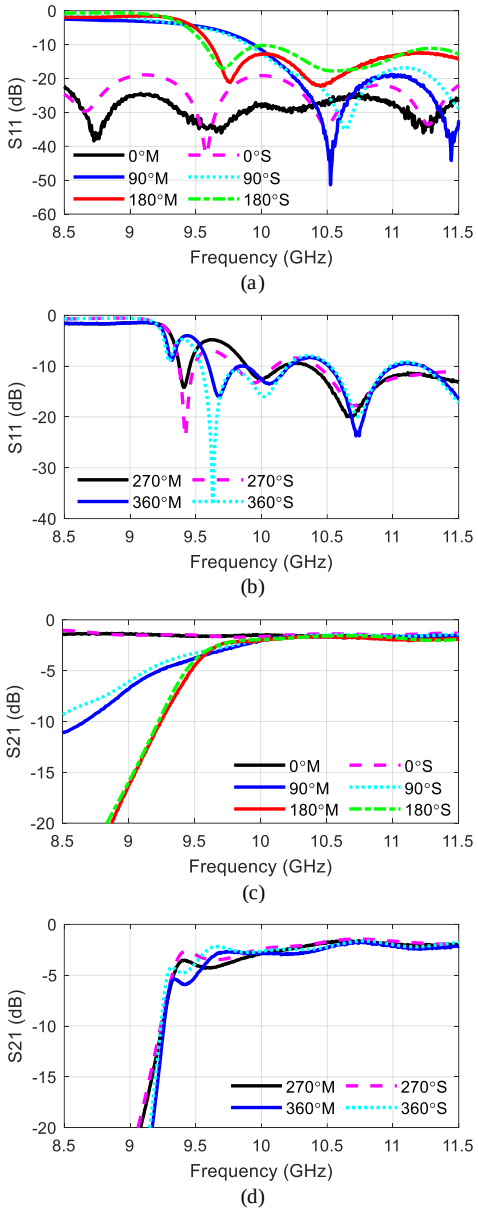

Fig. 11. The Measured S-parameter of the proposed phase shifter with non-uniform LM via. (a)-(b) S_{11} and (c)-(d) S_{21}. [M: is for measurement results and S is for simulated results]

S_{11} and S_{21} performance of the proposed phase shifter. S_{22} and S_{12} were also measured and found to be the mirror images of S_{11} and S_{21}, and hence for brevity they are not shown in this paper. The proposed phase shifter achieves a total measured phase shift of 368.6°, when all of the LM vias are active. This compares to a simulated phase shift of 360.5°. The proposed phase shifter has an IL of lower than 2.8 dB for all states, as shown in Fig. 9. A good standard of agreement was observed between the simulated and measured phase results. The detailed phase and IL results, at 10 GHz, are summarized in TABLE III. The size of the measured phase steps is 47° ± 3.3°, except for state 7 which has a measured phase step of 53.1°, in comparison to a simulated value of 47.5°. The discrepancies between the measured and simulated phase shift are mainly attributable to combination of fabrication tolerances, especially in the position and the size of each via hole. Simulation results shows that the

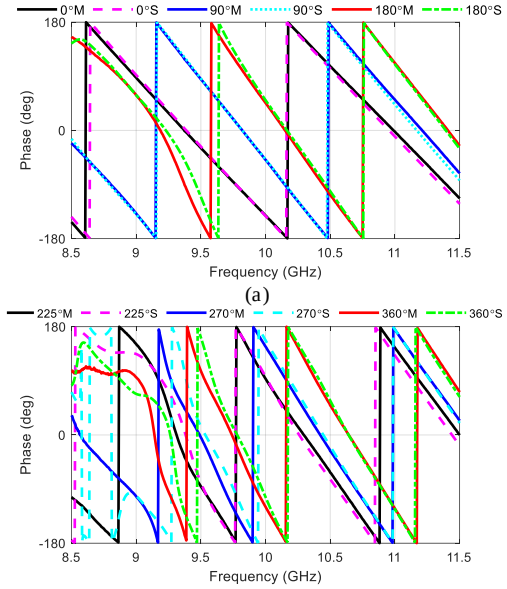

Fig. 12. The Measured S_{21} of the proposed uniform LM phase shifter. (a) 0° to 180° and (b) 180° to 360°. [M: is for measurement results and S is for simulated results]

TABLE IV.
Measured phases of the proposed phase shifter at 10 GHz

State	Number of active LM vias	Simulated total phase shift (step)	Measured total phase shift (step)	Measured IL (dB)
State 1 (S1)	0	0	0	1.4
State 2 (S2)	1	35° (35°)	34° (34°)	3.1
State 3 (S3)	2	92° (57°)	92.5° (58.5°)	2.7
State 4 (S4)	3	139.4 (47.4°)	136.5° (44°)	2.6
State 5 (S5)	4	181.4 (42°)	187° (50.5°)	3
State 6 (S6)	5	223.4° (42°)	234.8° (47.8°)	2.2
State 7 (S7)	6	275.4° (52°)	285.8° (51.0°)	2.6
State 8 (S8)	7	319.4° (44°)	332.7° (46.9°)	1.9
State 9 (S9)	8	363.4° (44°)	379.5° (46.5°)	3.1
	Total	363.4°	379.5	

phase of the proposed phase shifter is sensitive to the position of LM vias (*Yc*) and *x2* to *x8*. For example, a fabrication error of 0.1 mm in position of *Yc* for all eight LM vias could result in a phase change up to ≈27°, while a fabrication error of 0.05mm in *Yc* could lead to a total phase change of ≈13°. However, a 0.1 mm fabrication tolerance in all $x2$ to $x8$ position could result up to 8.5° of phase change, while a fabrication error of 0.05mm in *Yc* could produce a total phase change of ≈5°. In addition, we observe a small frequency shift (of ≈50MHz to ≈75 MHz) between key features in the simulated and measured magnitude of S_{11} and S_{21}, as shown in Figs. 8 and 9. This can be attributed to the tolerance in the positions of LM vias and fabrication tolerances in the size of the SIW transmission line and the SIW to microstrip transition.

The IL of the proposed phase shifter can mainly be attributed to matching and dissipation losses within the substrate. For instance, in state 0 and at 10 GHz, the phase shifter has a simulated and measured IL of 1.65 dB together with an average of IL of 1.6 dB, over the entire operating band. This IL can be attributed to dissipation losses within the substrate due to the large electrical length of the phase shifter (L ≈ 2λ, where λ is the operation wavelength at 10 GHz). Finally, LM was modelled as a lossy metal having a conductivity of 3.4×10^6

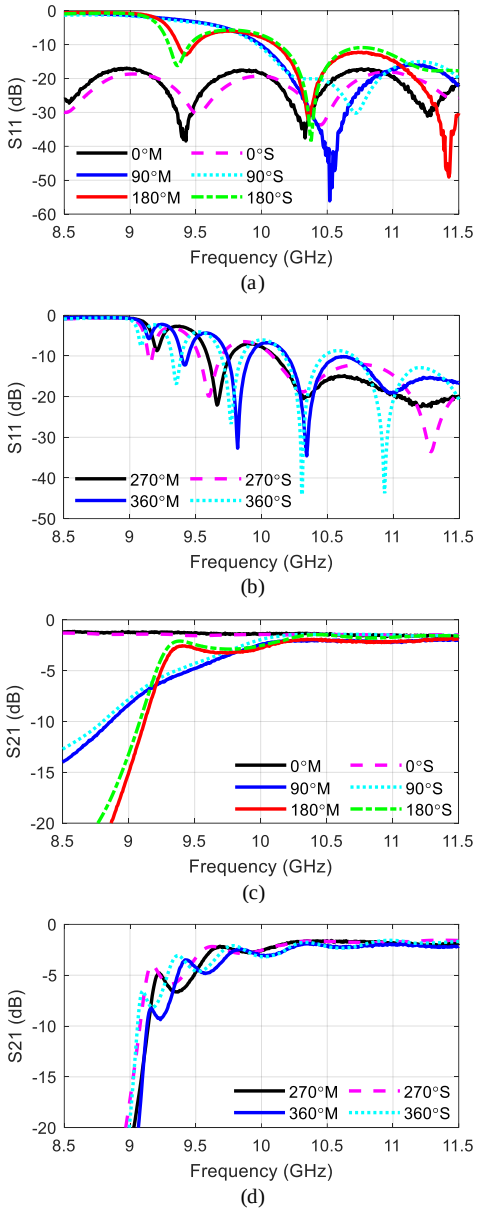

Fig. 13. The Measured S-parameter of the proposed phase shifter with uniform LM via. (a)-(b) S_{11} and (c)-(d) S_{21}. [M: is for measurement results and S is for simulated results]

S/m [77]. The conductivity of LM is relatively high. The conductivity of Copper is just 17 times higher than that of LM. In fact, due to high conductivity of LM there is no discernable difference between the performance of phase shifters having copper vias and that of a phase shifter having LM vias.

B. Phase shifter with uniform distance between the LM vias

The measured results for the proposed phase shifter having a uniform distance between vias are shown in Figs. 10 and Fig. 11 and are summarized in TABLE. IV. The total simulated phase shift which can be achieved using eight LM vias is 363.4° and the total measured phase shift is 379.5° as shown in Fig.10. In all states and at 10 GHz, the phase shifter has a measured IL lower than 3.2 dB, as shown in Fig. 11 and summarized TABLE. IV.

Fig. 12 shows the relative change in phase (i.e. the phase flatness) for the eight operating states of the proposed phase

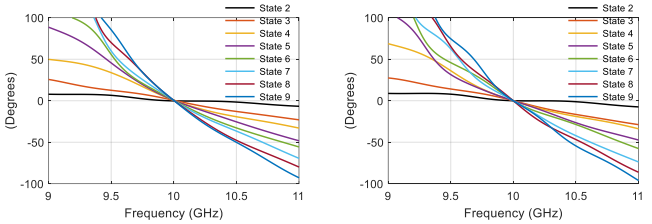

Fig. 14. Normalized change in the phase of the liquid metal phase shifters. (a) Non-uniform phase shifter, (b) Uniform phase shifter.

TABLE V.
MEASURED RMS BANDWIDTH OF PROPOSED PHASE SHIFTERS (UNIT: GHZ)

	Non- Uniform ±10° (GHz)	Uniform ±10° (GHz)	Non- Uniform ±20° (GHz)	Uniform ±20° (GHz)
State 2	<2.80 (8.70-11.50)	2.60 (8.90-11.50)	> 4 (8.0-12.0)	> 4 (8.0-12.0)
State 3	1.50 (9.35-10.85)	1.40 (9.40-10.80)	2.9 (8.90-11.80)	2.6 (9.0 -11.60)
State 4	0.9 (9.70-10.60)	1.00 (9.60-10.60)	1.45 (9.55-11.0)	1.5 (9.50-11.0)
State 5	0.75 (9.75-10.55)	0.75 (9.65-10.50)	1.1 (9.65-10.75)	1.15 (9.55-10.7)
State 6	0.65 (9.75-10.40)	0.70 (9.80-10.50)	0.8 (9.70-10.50)	0.9 (9.65-10.55)
State 7	0.50 (9.80-10.30)	0.45 (9.80-10.25)	0.7 (9.75-10.45)	0.65 (9.7-10.35)
State 8	0.40 (9.85-10.25)	0.40 (9.80-10.20)	0.55 (9.75-10.30)	0.5 (9.80-10.30)
State 9	0.3 (9.85-10.15)	0.25 (9.9-10.15)	0.45 (9.80-10.25)	0.45 (9.80-10.25)

shifter. In addition, the phase flatness of the proposed phase shifter was characterized. The bandwidth of the phase shifter can be described in terms of ±10° and ± 20° root mean square (RMS) change in the phase. These phase flatness figures are summarized in TABLE V. Fig. 12 and TABLE V show that the bandwidth of the proposed phase shifters varies according to the operating state. For example, between State 2 and State 5, there is a total phase shift of ~180°. For all of the states between State 2 and State 5 the ±10° RMS bandwidth of both phase shifters is higher than 750 MHz. The ±10° RMS bandwidth drops to ~650 MHz for State 6, while the bandwidth is ~400 MHz for State 8 and higher than 250 MHz for State 9. However, both proposed phase shifters have a measured ±20° RMS bandwidth higher than 400 MHz for all operation states between State 6 and State 8 and a bandwidth higher than 1.1 GHz for all states between State 2 and State 5, as summarized in TABLE V.

A single LM via behaves as a resonator within a high pass filter, as mentioned in Section III. The 3 dB cut-off frequency of the filter, thus formed, varies for each state and lies between 9.4 GHz and 9.8 GHz for most states, as shown in Figs. 9 and 11. For this reason the BW of the proposed phase shifter is asymmetric around 10 GHz. The proposed phase shifters therefore yield better performance at frequencies above 10 GHz, as shown in the S_{21} amplitude and phase plots given in Figs. 8 to 11. The effect is particularly evident in states which provide a phase shift higher than 180°. For instance, in the performance of both phase shifters one can observe distortion in the phase response at frequencies below ≈9.5 GHz. This is particularly true in states 6,7,8 and 9, as shown in Figs. 8b and 10b. However, due to the asymmetry mentioned above the

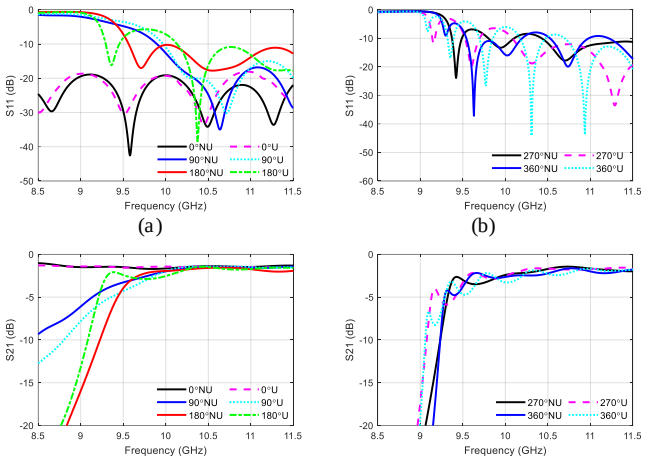

Fig. 15. Comparison between the simulated results of uniform phase shifter and non-uniform phase shifter. (a)-(b) S_{11} and (b) –(c) S_{21} [Caption: NU = Non-Uniform, U = Uniform]

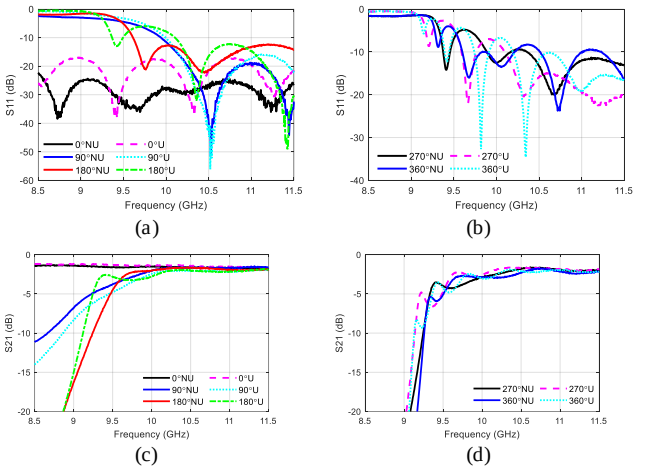

Fig. 16. Comparison between the measured results of uniform phase shifter and non-uniform phase shifter. (a)-(b) S_{11} and (b) –(c) S_{21} [Caption: NU = Non-Uniform, U = Uniform]

phase shifters do not exhibit such distortion at frequencies above than 10.5 GHz.

One of the possible approaches for improving the operating frequency bandwidth of the phase shifters would be to introduce a second set of 8 drill holes, designed to provide a phase shifting range of 360°, at a frequency close to 10 GHz (say 9 GHz or 11 GHz). If the operating frequency, of the second set of drill holes, were close enough to the operating frequency of the first set of drill holes then this should have the effect of creating a second pole in the S_{21} curve. This in turn would broaden the operating frequency bandwidth of the phase shifter. The disadvantage of this approach, however, is that it would increase the overall number of LM vias needed and thus the complexity of the design. An alternative approach for improving the bandwidth and IL performance of the proposed phase shifter is to design a new phase shifter having a phase step less than 45°. For example, preliminary simulation results shows that the bandwidth of the proposed phase shifter can be improved by more than 20%, in all operating states, when the proposed phase shifter has a phase step of 36° with 10 LM vias. Fig. 15 and Fig. 16 compare the performance of both of the

TABLE VI.
COMPARISON BETWEEN THE PERFORMANCE OF THE PROPOSED PHASE SHIFTERS AND OTHER PHASE SHIFTERS ACROSS DIFFERENT TECHNOLOGIES

Reference	Technology	Frequency (GHz)	FoM (°/dB)	IL (dB)	Phase shifting Range (°) ($\emptyset_{max}$)	BW (GHz)	RMS phase error (°)	RMS amplitude error (dB)	Resolution (°)	Size (mm)
[9]	0.25 μm SiGe BiCMOS	10	< 30	> 12	360	8.2-12	6.4	>3.0	11.25	1.87× 0.88
[15]	0.18μm SiGe BiCMOS	10	30.25	11.9	360	8-12	4.6	≈0.6	5.625	NA
[16]	250nm SiGe BiCMOS	10	27.7	≈13	360	8-12	4	≈0.6	5.625	3.42 × 0.95
[57]	0.13μm CMOS	10	27.3	13.2	360	8.5-10.5	4.1	≈0.8	5.625	2.06 × 0.58
[18]	Ferroelectric based	10	52	<8	342	8-10	8.5	>2.5	NA	2.8 × 3
[21]	Ferroelectric based	10	40.1	10.3	413	8-12	NA	>3	NA	3.8 × 2.3
[25]	Ferrite - LTCC	10.6	48	<7	215	9-12	NA	NA	NA	≈45 × 45
[27]	Liquid Crystal	10	≈24	≈2.5	≈60	10-67	NA	NA	NA	NA
[41]	Liquid Crystal	14.8	NA	NA	185	14.5-15.3	NA	NA	NA	NA
[42]	Liquid Crystal	10	≈15.2	≈5	≈101	6-10	NA	NA	NA	NA
[44]	Liquid Crystal	10	NA	≈3.9	≈100	5-40	NA	>3	NA	< 4 × 1
[7]	GaN	10	12.8	14	180	8.5-11.5	4.5	≈0.6	11.25	4.7 × 5
[54]	GaN	10	≈11	<5	22.5 or 45	7.5-13	≈5.6	1.1	NA	≈1 × 1
[66]	5 bit MEMS	10	≈60	≈6	360	8-12	<10	>4	11	≈9 × 1.2
[79]	Liquid Metal	5.6	70	≈1	≈67	NA	NA	NA	NA	NA
[80]	Liquid Metal	10	78.3	2.3	180	9.8-10.2	10	NA	10	87.2 × 56.2
[107]	PIN Diode - SIW	10	≈90	≈2	<180	10-14	NA	>0.8	NA	NA
This work	Liquid Metal(Non-Uniform)	10	131.3	<2.8	367.6	9.8-10.25	20	<1.5	≈45	57.2 × 14
This work	Liquid Metal(Uniform)	10	122.4	<3.1	379.5	9.8-10.25	20	<1.5	≈45	57.2 × 14

proposed phase shifters. From inspection of the overlaid curves one can observe very little difference between the performance of the two phase shifters. This is especially true of the insertion loss performance, as shown in Figs. 15(b), 15(d), 16(b), and 16(d). For instance, the variation in IL performance between any two similar states in both of the proposed phase shifters is less than 0.5 dB, across the entire operating bandwidth. The reason for the similarities in the performance of the proposed phase shifters is that they have similar reflection coefficients (S_{11} and S_{22}) for each state, as shown in Figs. 15(a), (b) and Fig. 16(a), (b). The IL performance is directly affected by the impedance mismatch (as measured by the S_{11} and S_{22} values). Furthermore, if their $|S_{11}|$ and $|S_{22}|$ is greater than 6 dB, then both phase shifters will have low and similar IL performance. The difference in IL will be much less when the $|S_{11}|$ and $|S_{22}|$ is greater than 10 dB. Finally, the difference in IL becomes negligible when the $|S_{11}|$ and $|S_{22}|$ is greater than 15 dB.

VI. BENCHMARKING

This section compares the performance of the proposed phase shifter against that of phase shifters based on with alternative state-of-the-art technologies. It also discusses the advantages and disadvantages of the proposed phase shifters. Table VI compares the performance of the proposed liquid metal (LM) phase shifter against that of several state-of-the-art X-band phase shifters. The proposed LM phase shifters have low IL and low RMS amplitude variations (<1.5 dB for all states). The IL performance of the proposed phase shifters is better (i.e. lower) than that of all of the state-of-the-art phase shifters which provide a phase shift of up to 360°. This enables the proposed phase shifters to have an extraordinary FoM performance of 131.3 °/dB and 122.4 °/dB at 10 GHz. This FoM is significantly higher (i.e. better) than that of all state-of-the-art phase shifters, irrespective of the technology used. In addition, the proposed phase shifters are based on SIW technology and fed using SMA connectors. We expect that the proposed phase shifters are capable of handling very levels of RF power. The reason for this is that there appears to be nothing about LM that should limit its power handling capability. The power handling capability of the phase shifters is likely to be limited only by that of the SIW transmission line itself, which is considerable. Furthermore, in comparison, to the LM phase shifters proposed in [79] and [80], the proposed phase shifters have much better FoM performance together with a larger overall phase shift of 360°, in comparison to 67° for [79], and 180° for [80]. In addition, the proposed phase shifters have wider operating bandwidth than [80]. Specifically, the phase shifter reported in [80] has a $\pm$10° RMS bandwidth of ≈440 MHz with total phase shift of 180°. The proposed phase shifters, on the other hand, have $\pm$10° RMS bandwidth wider than 750 MHz when achieving a phase shift of 180°. This involves reconfiguring between State 1 and State 5, as summarized in Table V. Finally, in comparison, to [80], the proposed phase shifter is less complex with much fewer LM vias. They are also much smaller in size and most importantly have the ability to be easily integrated an SIW feeding structure to realize a complete phased array system. This is one of the key motivations for developing the proposed phase shifters. However, the phase shifter reported in [80] relies on switching between different SIW transmission lines that have different electrical length to achieve the phase shift which requires large physical size to allow the phase shifter to accommodate the different physical paths. This limits the capability of the phase shifter in [80] to be integrated in a feeding structure suitable for a complete phased array antenna system based on LM technology.

However, the main disadvantage of the proposed phase shifters that they have limited $\pm$20° RMS bandwidth of 400 MHz together with relatively coarse resolution, of 45°, and a relatively larger physical size. For instance, in comparison to

the proposed LM phase shifter, the CMOS and GaN based phase shifters, report in [9], [15], [16], [57], [7], [54], all have a much better resolution, wider bandwidth, and smaller in size. However, they have much worst FoM and IL performance and they suffer from limited power handling capability in comparison to the proposed LM phase shifters. Finally, the proposed phase shifter is expected to have a reconfiguration time ranges between milliseconds to seconds [55], [81]. For example, Liquid metal actuation speeds of up to 30 cm/s have been reported in the literature when using electrochemically controlled capillary (ECC) action [108]. It would thus take approximately 3 ms to fill each via using ECC action. This is relatively slow in comparison with phase shifter based on competing technologies. However, with further developments, actuation speeds are likely to increase.

VII. Conclusion

This paper presents two phase shifters. The phase shifters compact and they are based on substrate integrated waveguide (SIW) technology, which makes them suitable for use within phased array antennas. The paper presents a design process for those phase shifters along with the simulated and the experimentally validated results for a hardware prototype. The phase shifters can be reconfigured using vias formed of liquid metal (LM). The proposed phase shifters exhibit a 360° phase shifting range along with low insertion loss (IL). In the proposed designs, LM is used to create removable vias, which can be used to reconfigure the phase of the proposed phase shifters. Specifically, when a certain via is needed a drill hole is filled with LM. When the via is no longer needed the LM is removed. Each phase shifter incorporates a total of eight drill holes. Both phase shifters can achieve a total phase shifting range of ~360° in eight steps of ~45°. The proposed phase shifters offer various important advantages over the existing technology, including: low IL, excellent Figure of Merit (FoM), and the potential for high power handling ability.

Acknowledgement

We wish to acknowledge the kind support of Rogers Corporation who donated substrates used in the prototypes.

References

[1] J. P. Srarski, "Optimization of the matching network for a hybrid coupler phase shifter," *IEEE Trans. Microw. Theory Tech.*, vol. MTT-25, no. 8, pp. 662–666, Aug. 1977.

[2] R. P. Coats, "An octave-band switched-line microstrip 3-b diode phase shifter," *IEEE Trans. Microw. Theory Tech.*, vol. MTT-21, no. 7, pp. 444–449, Jul. 1973.

[3] J. F. White, "High power, p-i-n diode controlled, microwave transmission phase shifters," *IEEE Trans. Microw. Theory Tech.*, vol. MTT-13, no. 2, pp. 233–242, Mar. 1965.

[4] T. Djerafi, N. J. G. Fonseca and K. Wu, "Broadband Substrate Integrated Waveguide 4×4 Nolen Matrix Based on Coupler Delay Compensation," *IEEE Transactions on Microwave Theory and Techniques*, vol. 59, no. 7, pp. 1740-1745, July 2011.

[5] K. -J. Koh and G. M. Rebeiz, "0.13μm CMOS Phase Shifters for X-, Ku-, and K-Band Phased Arrays," *IEEE Journal of Solid-State Circuits*, vol. 42, no. 11, pp. 2535-2546, Nov. 2007.

[6] M. van Wanum, G. van der Bent, M. Rodenburg, and A. P. de Hek, "Generic robust LVCMOS-compatible control logic for GaAs HEMT switches," in *Proc. IEEE Eur. Microw. Integr. Circuits Conf.*, Sep. 2006, pp. 83–86.

[7] W. Luo, H. Liu, Z. Zhang, P. Sun and X. Liu, "High-Power X-Band 5b GaN Phase Shifter with Monolithic Integrated E/D HEMTs Control Logic," *IEEE Trans. Electron Devices*, vol. 64, no. 9, pp. 3627-3633, Sept. 2017.

[8] M. Teshiba, R. Van Leeuwen, G. Sakamoto, and T. Cisco, "A SiGe MMIC 6-bit PIN diode phase shifter," *IEEE Microw. Wireless Compon. Lett.*, vol. 12, no. 12, pp. 500–501, Dec. 2002.

[9] B. Cetindogan, E. Ozeren, B. Ustundag, M. Kaynak and Y. Gurbuz, "A 6 Bit Vector-Sum Phase Shifter with a Decoder Based Control Circuit for X-Band Phased-Arrays," *IEEE Microw. and Wireless Comp. Lett*, vol. 26, no. 1, pp. 64-66, Jan. 2016.

[10] Z. Duan, Y. Wang, W. Lv, Y. Dai and F. Lin, "A 6-bit CMOS Active Phase Shifter for Ku-Band Phased Arrays," *IEEE Microw. and Wireless Comp. Lett.*, vol. 28, no. 7, pp. 615-617, July 2018.

[11] T. Wu *et al*., "A Ku-Band 6-Bit Vector-Sum Phase Shifter with Half-Quadrant Control Technique," *IEEE Access*, vol. 8, pp. 29311-29318, 2020.

[12] M. Sayginer and G. M. Rebeiz, "An Eight-Element 2–16-GHz Programmable Phased Array Receiver with One, Two, or Four Simultaneous Beams in SiGe BiCMOS," *IEEE Trans. Microw. Theory Tech.*, vol. 64, no. 12, pp. 4585-4597, Dec. 2016.

[13] K. Xu, "Silicon electro-optic micro-modulator fabricated in standard CMOS technology as components for all silicon monolithic integrated optoelectronic systems", Journal of Microcmechanics and microengineering, vol. 31, 054001, April, 2021.

[14] K. Wu, H. Zhang, Y. Chen, Q. Luo and K. Xu, "All-Silicon Microdisplay Using Efficient Hot-Carrier Electroluminescence in Standard 0.18μm CMOS Technology," *IEEE Electron Device Letters*, vol. 42, no. 4, pp. 541-544, April 2021.

[15] Z. Li, J. Qiao and Y. Zhuang, "An X-Band 5-Bit Active Phase Shifter Based on a Novel Vector-Sum Technique in 0.18μm SiGe BiCMOS," *IEEE Trans. on Circuits and Sys. II: Express Briefs*, vol. 68, no. 6, pp. 1763-1767, June 2021

[16] A. Burak, C. Çalışkan, M. Yazici and Y. Gurbuz, "X-Band 6-Bit SiGe BiCMOS Multifunctional Chip with +12 dBm IP1dB and Flat-Gain Response," *IEEE Trans. on Circuits and Sys. II: Express Briefs*, vol. 68, no. 1, pp. 126-130, Jan. 2021.

[17] C. Liu *et al*., "A Fully Integrated X-Band Phased-Array Transceiver in 0.13μm SiGe BiCMOS Technology," *IEEE Trans. Microw. Theory Tech.*, vol. 64, no. 2, pp. 575-584, Feb. 2016.

[18] M. Sazegar *et al*., "Low-Cost Phased-Array Antenna Using Compact Tunable Phase Shifters Based on Ferroelectric Ceramics," *IEEE Trans. Microw. Theory Tech.*, vol. 59, no. 5, pp. 1265-1273, May 2011.

[19] W. Kim, M. F. Iskander and W. D. Palmer, "An Integrated Phased Array Antenna Design Using Ferroelectric Materials and the Continuous Transverse Stub Technology," *IEEE Trans. on Ant. and Propag.*, vol. 54, no. 11, pp. 3095-3105, Nov. 2006.

[20] Z. Zhao, X. Wang, K. Choi, C. Lugo and A. T. Hunt, "Ferroelectric Phase Shifters at 20 and 30 GHz," *IEEE Trans. Microw. Theory Tech.*, vol. 55, no. 2, pp. 430-437, Feb. 2007.

[21] M. Sazegar, Y. Zheng, H. Maune, C. Damm, X. Zhou and R. Jakoby, "Compact Tunable Phase Shifters on Screen-Printed BST for Balanced Phased Arrays," *IEEE Trans. Microw. Theory Tech.*, vol. 59, no. 12, pp. 3331-3337, Dec. 2011.

[22] W. Hu, D. Zhang, M. J. Lancaster, T. W. Button and B. Su, "Investigation of Ferroelectric Thick-Film Varactors for Microwave Phase Shifters," *IEEE Trans. Microw. Theory Tech.*, vol. 55, no. 2, pp. 418-424, Feb. 2007

[23] F. A. Ghaffar and A. Shamim, "A Partially Magnetized Ferrite LTCC-Based SIW Phase Shifter for Phased Array Applications," *IEEE Trans. Magn.*, vol. 51, no. 6, pp. 1-8, Jun. 2015.

[24] S. I. M. Sheikh *et al*., "Analog/Digital Ferrite Phase Shifter for Phased Array Antennas," *IEEE Ant. Wireless Propag. Lett.*, vol. 9, pp. 319-321, Feb. 2010.

[25] S. Kagita, A. Basu and S. K. Koul, "Characterization of LTCC-Based

Ferrite Tape in X-band and Its Application to Electrically Tunable Phase Shifter and Notch Filter," *IEEE Trans. Magn.*, vol. 53, no. 1, pp. 1-8, Jan. 2017.

[26] D. Wang, E. Polat, H. Tesmer, H. Maune and R. Jakoby, "Switched and Steered Beam End-Fire Antenna Array Fed by Wideband Via-Less Butler Matrix and Tunable Phase Shifters Based on Liquid Crystal Technology," *IEEE Trans. on Ant. and Propag*, doi: 10.1109/TAP.2022.3142334.

[27] D. Wang, E. Polat, H. Tesmer, R. Jakoby and H. Maune, "Highly Miniaturized Continuously Tunable Phase Shifter Based on Liquid Crystal and Defected Ground Structures," *IEEE Microwave and Wireless Comp. Lett.*, doi: 10.1109/LMWC.2022.3142410.

[28] X. Y. Li, D. Jiang, J. Liu and M. S. Tong, "A Ka-Band Multilayer Beaming-Scanning Antenna Using Liquid Crystals," *IEEE Antennas and Wireless Propagation Letters*, vol. 21, no. 1, pp. 44-48, Jan. 2022.

[29] C. Yang, C. Kuo, C. Tang, J. C. Chen, R. Pan and C. Pan, "Liquid-Crystal Terahertz Quarter-Wave Plate Using Chemical-Vapor-Deposited Graphene Electrodes," *IEEE Photonics Journal*, vol. 7, no. 6, pp. 1-8, Dec. 2015.

[30] A. K. Sahoo, C. Yang, O. Wada and C. Pan, "Twisted Nematic Liquid Crystal Based Terahertz Phase Shifter with Crossed Indium Tin Oxide Finger Type Electrodes," *IEEE Trans. on Terahertz Science and Tech.*, vol. 9, no. 4, pp. 399-408, July 2019.

[31] X. Wang *et al*., "Agile Laser Beam Deflection With High Steering Precision and Angular Resolution Using Liquid Crystal Optical Phased Array," *IEEE Trans. on Nanotechnology*, vol. 17, no. 1, pp. 26-28, Jan. 2018.

[32] A. Alex-Amor *et al*., "Analytical Approach of Director Tilting in Nematic Liquid Crystals for Electronically Tunable Devices," *IEEE Access*, vol. 7, pp. 14883-14893, 2019.

[33] R. Reese *et al*., "Liquid Crystal Based Dielectric Waveguide Phase Shifters for Phased Arrays at W-Band," *IEEE Access*, vol. 7, pp. 127032-127041, 2019.

[34] Y. Xing *et al*., "Digitally Controlled Phase Shifter Using an SOI Slot Waveguide with Liquid Crystal Infiltration," *IEEE Photonics Tech. Lett.*, vol. 27, no. 12, pp. 1269-1272, 15 June15, 2015

[35] M. Nickel *et al*., "Ridge Gap Waveguide Based Liquid Crystal Phase Shifter," *IEEE Access*, vol. 8, pp. 77833-77842, 2020.

[36] B. S. -Y. Ung *et al*., "Towards a Rapid Terahertz Liquid Crystal Phase Shifter: Terahertz In-Plane and Terahertz Out-Plane (TIP-TOP) Switching," *IEEE Transactions on Terahertz Science and Technology*, vol. 8, no. 2, pp. 209-214, March 2018.

[37] S. -Y. Sun *et al*., "Electronically Tunable Liquid-Crystal-Based F-Band Phase Shifter," *IEEE Access*, vol. 8, pp. 151065-151071, 2020.

[38] Tsong-Ru Tsai, Chao-Yuan Chen, Ru-Pin Pan, Ci-Ling Pan and Xi-Cheng Zhang, "Electrically controlled room temperature terahertz phase shifter with liquid crystal," *IEEE Microw. and Wireless Comp. Lett*, vol. 14, no. 2, pp. 77-79, Feb. 2004.

[39] Y. Utsumi, T. Kamei, K. Saito and H. Moritake, "Increasing the speed of microstrip-line-type polymer-dispersed liquid-crystal loaded variable phase shifter," *IEEE Trans. Microw. Theory Tech.*, vol. 53, no. 11, pp. 3345-3353, Nov. 2005.

[40] Hsin-Ying Wu, Cho-Fan Hsieh, Tsung-Ta Tang, Ru-Pin Pan and Ci-Ling Pan, "Electrically tunable room-temperature 2/spl pi/ liquid crystal terahertz phase shifter," *IEEE Photonics Technology Letters*, vol. 18, no. 14, pp. 1488-1490, July 2006.

[41] Y. Zhao, C. Huang, A. Qing and X. Luo, "A Frequency and Pattern Reconfigurable Antenna Array Based on Liquid Crystal Technology," *IEEE Photonics Journal*, vol. 9, no. 3, pp. 1-7, June 2017.

[42] C. Ding, F. -Y. Meng, J. -Q. Han, H. -L. Mu, Q. -Y. Fang and Q. Wu, "Design of Filtering Tunable Liquid Crystal Phase Shifter Based on Spoof Surface Plasmon Polaritons in PCB Technology," *IEEE Trans. on Comp., Packaging and Manufacturing Tech.*, vol. 9, no. 12, pp. 2418-2426, Dec. 2019.

[43] T. Kuki, H. Fujikake and T. Nomoto, "Microwave variable delay line using dual-frequency switching-mode liquid crystal," *IEEE Trans. Microw. Theory Tech.*, vol. 50, no. 11, pp. 2604-2609, Nov. 2002.

[44] A. Franc, O. H. Karabey, G. Rehder, E. Pistono, R. Jakoby and P. Ferrari, "Compact and Broadband Millimeter-Wave Electrically Tunable Phase Shifter Combining Slow-Wave Effect with Liquid Crystal Technology," *IEEE Trans. Microw. Theory Tech.*, vol. 61, no. 11, pp. 3905-3915, Nov. 2013.

[45] S. Hayden and G. M. Rebeiz, "2-bit MEMS distributed X-band phase shifters," *IEEE Microw. Guided Wave Lett.*, vol. 10, no. 12, pp. 540-542, Dec. 2000.

[46] A. E. Martynyuk, A. G. Martinez-Lopez and J. I. Martinez Lopez, "2-bit X-Band Reflective Waveguide Phase Shifter with BCB-Based Bias Circuits," *IEEE Trans. Microw. Theory Techn.*, vol. 54, no. 12, pp. 4056-4061, Dec. 2006.

[47] B. T. W. Gillatt, M. D'Auria, W. J. Otter, N. M. Ridler and S. Lucyszyn, "3-D Printed Variable Phase Shifter," *IEEE Microw. Wireless Compon. Lett.*, vol. 26, no. 10, pp. 822-824, Oct. 2016.

[48] J. J. P. Venter, T. Stander and P. Ferrari, "X-Band Reflection-Type Phase Shifters Using Coupled-Line Couplers on Single-Layer RF PCB," *IEEE Microw. Wireless Compon. Lett.*, vol. 28, no. 9, pp. 807-809, Sept. 2018.

[49] M. A. Morton, J. P. Comeau, J. D. Cressler, M. Mitchell and J. Papapolymerou, "5 bit, silicon-based, X-band phase shifter using a hybrid pi/t high-pass/low-pass topology," *IET Microw. Ant. & Propag.*, vol. 2, no. 1, pp. 19-22, Feb. 2008.

[50] Y. Du, J. Bao and X. Zhao, "5-bit MEMS distributed phase shifter," *IET Electr. Lett.*, vol. 46, no. 21, pp. 1452-1453, Oct. 2010.

[51] Guan-Leng Tan, R. E. Mihailovich, J. B. Hacker, J. F. DeNatale and G. M. Rebeiz, "A 2-bit miniature X-band MEMS phase shifter," *IEEE Microw. Wireless Compon. Lett.*, vol. 13, no. 4, pp. 146-148, Apr. 2003.

[52] K. Gharibdoust, N. Mousavi, M. Kalantari, M. Moezzi and A. Medi, "A Fully Integrated 0.18 CMOS Transceiver Chip for X-Band Phased-Array Systems," *IEEE Trans. Microw. Theory Techn.*, vol. 60, no. 7, pp. 2192-2202, Jul. 2012.

[53] M. Cho, D. Baek and J. Kim, "An X-Band 5 Bit Phase Shifter With Low Insertion Loss in 0.18μm SOI Technology," *IEEE Microw. Wireless Compon. Lett.*, vol. 22, no. 12, pp. 648-650, Dec. 2012.

[54] T. N. Ross, K. Hettak, G. Cormier and J. S. Wight, "Design of X-Band GaN Phase Shifters," *IEEE Trans. Microw. Theory Techn.*, vol. 63, no. 1, pp. 244-255, Jan. 2015.

[55] A. Qaroot and G. Mumcu, "Microfluidically Reconfigurable Reflection Phase Shifter," *IEEE Microw. Wireless Compon. Lett.*, vol. 28, no. 8, pp. 684-686, Aug. 2018.

[56] S. Yeo, J. Chun and Y. Kwon, "A 3-D X-Band T/R Module Package with an Anodized Aluminum Multilayer Substrate for Phased Array Radar Applications," *IEEE Trans. Adv. Packag.*, vol. 33, no. 4, pp. 883-891, Nov. 2010.

[57] S. Sim, L. Jeon and J. Kim, "A Compact X-Band Bi-Directional Phased-Array T/R Chipset in 0.13 μm CMOS Technology," *IEEE Trans. Microw. Theory Techn.*, vol. 61, no. 1, pp. 562-569, Jan. 2013.

[58] C. Chang *et al*., "A New Compact High-Power Microwave Phase Shifter," *IEEE Trans. Microw. Theory Techn.*, vol. 63, no. 6, pp. 1875-1882, Jun. 2015.

[59] B. Acikel, T. R. Taylor, P. J. Hansen, J. S. Speck and R. A. York, "A new high performance phase shifter using Ba/sub x/Sr/sub 1-x/TiO3 thin films," *IEEE Microw. Wireless Compon. Lett.*, vol. 12, no. 7, pp. 237-239, Jul. 2002.

[60] S. Kagita, A. Basu and S. K. Koul, "Characterization of LTCC-Based Ferrite Tape in X-band and Its Application to Electrically Tunable Phase Shifter and Notch Filter," *IEEE Trans. Magn.*, vol. 53, no. 1, pp. 1-8, Jan. 2017.

[61] Zhang Jin, S. Ortiz and A. Mortazawi, "Design and performance of a new digital phase shifter at X-band," *IEEE Microw. Wireless Compon. Lett.*, vol. 14, no. 9, pp. 428-430, Sept. 2004.

[62] D. J. Chung, R. G. Polcawich, J. S. Pulskamp and J. Papapolymerou, "Reduced-Size Low-Voltage RF MEMS X-Band Phase Shifter Integrated on Multilayer Organic Package," *IEEE Trans. Compon., Packag. and Manuf. Technol.*, vol. 2, no. 10, pp. 1617-1622, Oct. 2012.

[63] R. Ramadoss, A. Sundaram and L. M. Feldner, "RF MEMS phase shifters based on PCB MEMS technology," *IET Elect. Lett.*, vol. 41, no. 11, pp. 654-656, May 2005.

[64] Sarah N. McClung, Shahrokh Saeedi, Hjalti H. Sigmarsson, "Band-Reconfigurable Filter With Liquid Metal Actuation," *IEEE Trans. Microw. Theory Techn.*, vol. 66, no. 6., pp. 3073-3080. Jun. 2018.

[65] M. Cho, D. Baek and J. Kim, "An X-Band 5 Bit Phase Shifter With Low Insertion Loss in 0.18 μm SOI Technology," *IEEE Microwave and Wireless Components Letters*, vol. 22, no. 12, pp. 648-650, Dec. 2012.

[66] M. A. Morton and J. Papapolymerou, "A Packaged MEMS-Based 5-bit X-Band High-Pass/Low-Pass Phase Shifter," *IEEE Transactions on Microwave Theory and Techniques*, vol. 56, no. 9, pp. 2025-2031, Sep. 2008.

[67] S. Gevorgian, *Ferroelectrics in Microwave Devices, Circuits and Systems: Physics, Modeling, Fabrication and Measurements*. Berlin, Germany: Springer, 2009.

[68] Jonathan H. Dang, Ryan C. Gough, Andy M. Morishita, Aaron T. Ohta, Wayne A. Shiroma, "A Tunable X-Band Substrate Integrated Waveguide Cavity Filter using Reconfigurable Liquid-Metal Perturbing Posts," in *IEEE MTT-S Int. Microw. Symp. (IMS)*, 2015.

[69] Sarah N. McClung, Shahrokh Saeedi, Hjalti H. Sigmarsson, "Single-Mode-Dual-Band to Dual-Mode-Single-Band Bandpass Filter with Liquid Metal," in Proc. *IEEE 18th Wireless and Microw. Technol. Conference (WAMICON)*, 2017.

[70] Alex H. Pham, Shahrokh Saeedi, Hjalti H. Sigmarsson, "Continuously-Tunable Substrate Integrated Waveguide Bandpass Filter Actuated by Liquid Metal," in Proc. *IEEE MTT-S Int. Microw. Symp. (IMS)*, 2019.

[71] Tahar Ben Chaieb, Abdelkhalek Nasri, Hassen Zairi, "Liquid filled method for Substrate Integrated Waveguide reconfigurable filter," in Proc. *Int. Conference on Adv. Sys. and Electric Technol. (IC_ASET)*, 2018.

[72] Sabreen Khan, Nahid Vahabisani, Mojgan Daneshmand, "A Fully 3-D Printed Waveguide and Its Application as Microfluidically Controlled Waveguide Switch," *IEEE Trans. Compon., Packag. and Manuf. Technol.*, vol. 7, no. 1, pp. 70-80, Jan. 2017.

[73] Nahid Vahabisani, Sabreen Khan, Mojgan Daneshmand, "A K-Band Reflective Waveguide Switch Using Liquid Metal," *IEEE Antennas Wireless Propag. Lett.*, vol. 16, pp. 1788-91, Mar. 2017.

[74] S. Alkaraki, J. Kelly, A. L. Borja, R. Mittra and Y. Wang, "Gallium-Based Liquid Metal Substrate Integrated Waveguide Switches," *IEEE Microw. and Wireless Compon. Lett.*, vol. 31, no. 3, pp. 257-260, Mar. 2021.

[75] Meng Wang, Ian M. Kilgore, Michael B. Steer, Jacob J. Adams, "Characterization of Intermodulation Distortion in Reconfigurable Liquid Metal Antennas," *IEEE Antennas Wireless Propag. Lett.*, vol. 17, no. 2, pp. 279-82, Feb. 2018.

[76] Andy M. Morishita, Carolynn K. Y. Kitamura, Aaron T. Ohta, Wayne A. Shiroma, "A Liquid-Metal Monopole Array with Tunable Frequency, Gain, and Beam Steering," *IEEE Antennas Wireless Propag. Lett.*, vol. 12, no. pp. 1388-91, Oct. 2013.

[77] Cong Wang, Joo Chuan Yeo, Hui Chu, Chwee Teck Lim, Yong-Xin Guo, "Design of a Reconfigurable Patch Antenna Using the Movement of Liquid Metal," *IEEE Antennas Wireless Propag. Lett.*, vol. 17, no. 6, pp. 974-977, Jun. 2018.

[78] M. Wang, C. Trlica, M. R. Khan, M. D. Dickey, and J. J. Adams, "A reconfigurable liquid metal antenna driven by electrochemically controlled capillarity," *J. Appl. Phys.*, vol. 117, no. 19, May. 2015.

[79] J. H. Dang, R. C. Gough, A. M. Morishita, A. T. Ohta and W. A. Shiroma, "Liquid-metal-based phase shifter with reconfigurable EBG filling factor," in Proc. *IEEE MTT-S Int. Microw. Symp.*, Phoenix, AZ, 2015, pp. 1-4.

[80] S. Alkaraki, A. L. Borja, J. R. Kelly, R. Mittra and Y. Gao, "Reconfigurable Liquid Metal-Based SIW Phase Shifter," in *IEEE Transactions on Microwave Theory and Techniques*, vol. 70, no. 1, pp. 323-333, Jan. 2022.

[81] A. Dey and G. Mumcu, "Microfluidically Controlled Frequency Tunable Monopole Antenna for High-Power Applications," *IEEE Antennas Wireless Propag. Lett.*, vol. 15, pp. 226-229, 2016.

[82] K. Sellal, L. Talbi, T.A. Denidni, J. Lebel, "Design and implementation of substrate integrated waveguide phase shifter," *IET Microwave, Ant. & Prop., Vol.2, pp. 194- 197, Mar. 2008.*

[83] K. Hettak, G. A. Morin and M. G. Stubbs, "A novel miniature CPW topology of a high-pass/low-pass T-network phase shifter at 30 GHz," *2009 European Microwave Conference (EuMC)*, 2009, pp. 1140-1143.

[84] Koul, B., and Bhat, S.: "Microwave and millimeter wave phase shifters", (Artech House, 1991), vol. 2, pp. 411-414.

[85] T. A. Abele, "Inductive post arrays in rectangular waveguide," *The Bell System Technical Journal*, vol. 57, no. 3, pp. 577-594, Mar. 1978.

[86] Y. Leviatan, P. G. Li, A. T. Adams and J. Perini, "Single-Post Inductive Obstacle in Rectangular Waveguide," *IEEE Transactions on Microwave Theory and Techniques*, vol. 31, no. 10, pp. 806-812, Oct. 1983

[87] Markuvitz, N.: "Waveguide handbook" (Short Run Press Ltd, 1986).

[88] Young, L. Yan, W. Hong, K. Wu, and T. J. Cui, "Investigations on the propagation characteristics of the substrate integrated waveguide based on the method of lines," *IEE Proc. Microw., Antennas and Propag.*, vol. 152, no. 1, pp. 35–42, Feb. 2005. Doi:10.1049/ip-map:20040726

[89] J. E. Rayas-Sanchez and V. Gutierrez-Ayala, "A general EM-based design procedure for single-layer substrate integrated waveguide interconnects with microstrip transitions," *2008 IEEE MTT-S Int. Microwave Symp. Digest*, Atlanta, GA, USA, 2008, pp. 983-986.

[90] Feng Xu and Ke Wu, "Guided-wave and leakage characteristics of substrate integrated waveguide," in *IEEE Trans. on Microw. Theory Techn.*, vol. 53, no. 1, pp. 66-73, Jan. 2005.

[91] C. A. Balanis, "Arrays: Linear, Planar and Circular" in Antenna Theory, 4th Ed, Hobo-ken, NJ, USA: Wiley, 2005, ch. 6, pp. 285–368.

[92] W.-K. D. Deslandes, "Design equations for tapered microstrip-to-Substrate Integrated Waveguide transitions," in *IEEE MTT-S Int. Microw. Symp.*, Anaheim, CA, 2010, pp. 704-707.

[93] Cong Wang, Joo Chuan Yeo, Hui Chu, Chwee Teck Lim, Yong-Xin Guo, "Design of a Reconfigurable Patch Antenna Using the Movement of Liquid Metal," *IEEE Antennas Wireless Propag. Lett.*, Vol. 17, No. 6, 2018.

[94] W. Chen, Y. Li, R. Li, A. V. Thean and Y. Guo, "Bendable and Stretchable Microfluidic Liquid Metal-Based Filter," *IEEE Microw. Wireless Compon. Lett.*, vol. 28, no. 3, pp. 203-205, Mar. 2018.

[95] C. Koo, B. E. LeBlanc, M. Kelley, H. E. Fitzgerald, G. H. Huff and A. Han, "Manipulating Liquid Metal Droplets in Microfluidic Channels with Minimized Skin Residues Toward Tunable RF Applications," *Journal Microelectr. Sys.*, vol. 24, no. 4, pp. 1069-1076, Aug. 2015.

[96] M. A. Rafi, B. D. Wiltshire and M. H. Zarifi, "Wideband Tunable Modified Split Ring Resonator Structure Using Liquid Metal and 3-D Printing," *IEEE Microw. Wireless Compon. Lett.*, vol. 30, no. 5, pp. 469-472, May 2020.

[97] A. Ha and K. Kim, "Frequency tunable liquid metal planar inverted-F antenna," *IET Elect. Lett.*, vol. 52, no. 2, pp. 100-102, Jan. 2016.

[98] A. M. Watson *et al*., "Physically Reconfigurable RF Liquid Electronics via Laplace Barriers," *IEEE Trans. Microw. Theory Techn.*, vol. 67, no. 12, pp. 4881-4889, Dec. 2019.

[99] L. Song, W. Gao, C. O. Chui and Y. Rahmat-Samii, "Wideband Frequency Reconfigurable Patch Antenna with Switchable Slots Based on Liquid Metal and 3-D Printed Microfluidics," *IEEE Trans. Antennas Propag.*, vol. 67, no. 5, pp. 2886-2895, May 2019.

[100] T. Kim, K. Kim, S. Kim, J. Lee and W. Kim, "Micropatterning of Liquid Metal by Dewetting," *Journal Microelectr. Sys.*, vol. 26, no. 6, pp. 1244-1247, Dec. 2017.

[101] J. Low, P. Chee and E. Lim, "Deformable Liquid Metal Patch Antenna for Air Pressure Detection," *IEEE Sensors Journal*, vol. 20, no. 8, pp. 3963-3970, Apr. 2020.

[102] V. T. Bharambe, J. Ma, M. D. Dickey and J. J. Adams, "Planar, Multifunctional 3D Printed Antennas Using Liquid Metal Parasitics," *IEEE Access*, vol. 7, pp. 134245-134255, Sept. 2019.

[103] D. Rodrigo, L. Jofre and B. A. Cetiner, "Circular Beam-Steering Reconfigurable Antenna with Liquid Metal Parasitics," *IEEE Trans. Antennas Propag.*, vol. 60, no. 4, pp. 1796-1802, Apr. 2012.

[104] S. Singh et al., "A Pattern and Polarization Reconfigurable Liquid Metal Helical Antenna," in *IEEE Int. Symp. Antennas and Propag. & USNC/URSI National Radio Science Meeting*, Boston, MA, 2018, pp. 857-858.

[105] M. Wang, C. Trlica, M. R. Khan, M. D. Dickey, and J. J. Adams, "A reconfigurable liquid metal antenna driven by electrochemically controlled capillarity," *J. Appl. Phys.*, vol. 117, no. 19, May 2015.

[106] M. Wang, M. R. Khan, C. Trlica, M. D. Dickey, and J. J. Adams, "Pump free feedback control of a frequency reconfigurable liquid metal monopole," in Proc. *IEEE Int. Symp. Antennas Propag.*, 2015, pp. 2223–2224.

[107] B. Muneer, Z. Qi and X. Shanjia, "A Broadband Tunable Multilayer Substrate Integrated Waveguide Phase Shifter," *IEEE Microw. Wireless Compon. Lett.*, vol. 25, no. 4, pp. 220-222, Apr. 2015.

[108] Mohammad R. Khan, Chris Trlica, Michael D. Dickey, "Recapillarity: Electrochemically Controlled Capillary Withdrawal of a Liquid Metal Alloy from Microchannels," *Advanced Functional Materials*, Vol. 25, No. 5, pp. 671-678, Nov. 2014.